



Poly(lactic acid) (PLA)/poly(butylene succinate adipate) (PBSA) films with Micro fibrillated cellulose (MFC) and cardanol for packaging applications

Annalisa Apicella · Giovanna Molinari · Vito Gigante · Arianna Pietrosanto · Loredana Incarnato · Laura Aliotta · Andrea Lazzeri

Received: 30 April 2024 / Accepted: 15 August 2024
© The Author(s) 2024

Abstract Micro Fibrillated Cellulose (MFC) has emerged as a promising component in film formulations due to its unique barrier properties. In this study, to best of our knowledge, cardanol, a biobased plasticizer derived from cashew processing, was employed for the first time, as a dispersing aid for MFC, during a liquid assisted extrusion technique with a Poly(lactic acid) (PLA)/Poly(butylene succinate adipate) (PBSA) blend. The aim of the work is the production of PLA/PBSA/MFC films for packaging applications. The addition of different MFC amount was investigated (added at 0.5, 0.75 and 1 wt.% concentrations). The results obtained

are very interesting, in fact from one hand Cardanol improved the compatibility between PLA and PBSA and avoided the MFC agglomeration. On the other hand, micro fibrillated cellulose ensured a stable film blowing and the achievement of enhanced barrier properties, seal ability and mechanical resistance. In particular, the best result was obtained with an MFC content of 0.75 wt.% for which a good compromise in terms of films ductility, barrier properties and seal ability was achieved.

Keywords Biocomposites · Micro fibrillated cellulose · Polymeric films · Packaging applications

Annalisa Apicella and Giovanna Molinari have contributed equally to the work.

A. Apicella · G. Molinari · V. Gigante · L. Incarnato · L. Aliotta · A. Lazzeri
National Interuniversity Consortium of Materials Science and Technology (INSTM), 50121 Florence, Italy

A. Apicella · A. Pietrosanto · L. Incarnato
Department of Industrial Engineering, University of Salerno, 84084 Fisciano, Italy

G. Molinari · V. Gigante · L. Aliotta (✉) · A. Lazzeri
Department of Civil and Industrial Engineering, University of Pisa, 56122 Pisa, Italy
e-mail: laura.aliotta@unipi.it

G. Molinari
CNR-IPCF, National Research Council—Institute for Chemical and Physical Processes, 56124 Pisa, Italy

Introduction

For many years fossil-based polymers have been widely used in the packaging industry for different applications (films, pouches, rigid and foamed containers, etc.). However, growing fears on the environmental impact of the fossil-based polymers as well as the necessity to decrease the greenhouse gas emissions, has forced researchers and the industry to develop more sustainable packaging (Stark and Matuana 2021; Malafeev et al. 2023). In this context the use of biobased materials coming from renewable resources has gained much interest (Zinoviadou et al. 2016). Particular attention has been dedicated to find more sustainable solution in the packaging field due to its large plastic consumption (de Sousa 2021).

The movement towards more sustainable packaging solution requires the development on novel biobased materials together with the improvement of the existing ones (Dörnyei et al. 2023).

Among the biobased polymers, poly(lactic acid) (PLA) is the most attractive, being also available on the market with different grades customized for different structuring processes (Swetha et al. 2023). Although PLA exhibits good mechanical strength, printability and transparency, its barrier properties to gases and water vapor, ductility, processability and thermal stability are usually lower than conventional fossil-based plastics and fail to fully meet the demanding standards of many flexible packaging applications, among others, for food and beverages preservation (Apicella et al. 2018; Leneveu-Jenvrin et al. 2021; Samir et al. 2022; De Luca et al. 2023). The overcoming of PLA drawbacks can further widespread its application not only in the packaging sector (Qian and Sheng 2017).

At this purpose, to improve the PLA toughness and ductility, a possible strategy could be the reactive extrusion to develop block or random copolymers in melt compounding (Augé et al. 2023), or converting polymer blends into in situ composites through the formation of well-aligned micro/nanofibrils by virtue of such an external field, permitting the construction of strong dispersed phase and interfacial interaction (Evstatiev and Fakirov 1992; Xie et al. 2014). Nevertheless, an efficient low-cost technique, commonly adopted at industrial level, is the physical blending through twin-screw extrusion with a more ductile polymer (Nofar et al. 2019). Among the biodegradable and biobased polymers commercially available, the most interesting one, to be blended with PLA for flexible packaging applications, is the poly(butylene succinate co-adipate) (PBSA) (Aliotta et al. 2023a; Mastalygina and Aleksanyan 2023). Indeed, the PBSA good eco-efficiency coupled with its high availability, flexibility, excellent impact strength, as well as thermal and chemical resistance and good biodegradability (Changwichan et al. 2018) makes it an excellent candidate for the blending with PLA, as also demonstrated by a recent work in which extrusion processing parameter have been optimized with a DoE approach for the production of these blends (Gigante et al. 2023). Indeed, different successful studies can be found regarding the good flexibility reached with PLA/PBSA blends (Pivsa-Art et al.

2015; Lascano et al. 2019; Suwanamornlert et al. 2020; Aversa et al. 2022; Aliotta et al. 2023a). Therefore, PBSA is an excellent candidate to improve the PLA flexibility especially when its content is around 40 wt.%. For this PBSA content in fact, an improvement of the elongation up to 200% also accompanied by an increase in impact resistance three times higher than that of pure PLA have been reported (Aliotta et al. 2021).

Nevertheless, in some cases it is also necessary to improve the barrier properties and to reach this goal the use of suitable filler is necessary (Botta et al. 2021; Nath et al. 2023).

Cellulose can be used as filler to improve not only the barrier properties but also the mechanical ones (Kalia et al. 2011; Dufresne 2017). In particular, the unique properties of micro fibrillated cellulose (MFC) (high specific strength and modulus, high aspect ratio, light weight, low cost, biodegradability, and renewability) makes it very attractive to reinforce polymeric matrices (Li et al. 2021). The main issues to be faced on, are related to MFC drying, the incompatibility of hydrophilic cellulose and hydrophobic polymer matrices and the MFC agglomeration. In fact, being MFC generally produced in aqueous suspension, its drying leads to an irreversible agglomeration. Furthermore, it must be considered that the use of MFC suspensions during melting compound requires an efficient water removal to avoid the degradation of water sensible polymers (van den Oever et al. 2010; Lamm et al. 2021). An industrial sustainable technique to guarantee the MFC dispersion within the polymeric matrix and an efficient water removal, is the liquid assisted extrusion with the help of suitable plasticizer as MFC dispersing aids (Clemons and Sabo 2021). The incorporation of a suitable plasticizer into the MFC suspension has been proved to be a good solution to guarantee the MFC dispersion and at the same time to improve the processability. In literature several plasticizers have been successfully adopted like lactic acid oligomers (OLA), poly(ethylene glycol) (PEG), Triethyl citrate (TEC) (Paul et al. 2021; Molinari et al. 2021; Völtz et al. 2022; Aliotta et al. 2023b). However, the low molecular weight of these plasticizers can generate problems related to the plasticizer migration (Marcilla et al. 2017).

For the first time, the use of cardanol oil (CA) (derived from the side product of the cashew agro-industry) as MFC dispersing aid was investigated.

The molecular structure of cardanol oil make him less prone to its migration from the polymeric matrix (Mele et al. 2019). Cardanol is constituted by a mixture of phenolic compounds (Bloise et al. 2012) and thanks to the presence of the C15 chain attached to the meta-position of the phenolic ring, cardanol and its derivatives possess a relatively high solubility in non-polar environments and good processability. In addition, it has been observed that CA addition to a PLA matrix by hot melt extrusion has led to good results in terms of mechanical performance and processability (Hassouma et al. 2016; Greco et al. 2018; Mele et al. 2019). Moreover, it has been demonstrated that the cashew nut-derived oils can exert antioxidant and antibacterial properties (Andrade et al. 2011; Boonsai et al. 2014; Anand et al. 2015) making the use of CA oil more attractive.

In this work the attention was focused on the production and characterization of novel PLA/PBSA films containing different MFC amount (0.5–0.75 and 1 wt.%) and CA as dispersing aid. Based on previous studies of the same research group (Aliotta et al. 2021, 2023a) the ratio between the PLA/PBSA in the matrix was 60/40 (60 wt.% of PLA and 40 wt.% of PBSA), chosen based on the good ductility reached by this blend. The biocomposite were obtained by using the well-established wet extrusion compounding technique (Clemons and Sabo 2021) in which an emulsion containing MFC and CA was fed. The optimization of the temperature and venting of the extruder zones was carried out to achieve a complete water stripping. Subsequently the granules obtained with different MFC content, were again processed through film blowing technique and the obtained films were characterized from a morphological, mechanical, and thermal point of view. Then, by considering the possible applications of the obtained films for packaging sector, the barrier properties, contact angle and film seal ability were also explored.

Materials and methods

Materials

The materials used in this work are:

- Poly(lactic acid) (PLA), trade name Luminy LX175, purchased from Total Corbion PLA (Gorinchem, Netherlands). It is an extrusion grade PLA coming from natural resources having about 4% of D-lactic units [density: 1.24 g/cm³; melt flow index (MFI): 6 g/10 min at 210 °C and 2.16 kg].
- Poly(butylene succinate-co-adipate) (PBSA), trade name BioPBS FD92PM, purchased from Mitsubishi Chemical Corporation (Tokyo, Japan), is a copolymer of succinic acid, adipic acid and butandiol. This PBSA grade is tailored for both blown and cast film extrusion [density of 1.24 g/cm³; MFI: 4 g/10 min at 190 °C and 2.16 kg].
- Cardanol (CA) NC-514, provided by Cardolite (Gent, Belgium): is a di-functional glycidyl ether epoxy resin having a good reactivity. The chain of 8 carbons separating the aromatic groups allows to increase the flexibility processability [Epoxy Equivalent Weight: 490; viscosity at 25 °C: 25,000 cPs; density at 25 °C: 8.75 g/cm³].
- Micro Fibrillated Cellulose (MFC), trade name Exilva F 01-L 10%, provided by Borregaard (Sarpsborg, Norway) with a solid content of 1.5–2.4% (viscosity—in H₂O 2wt.%—≥ 14,000 mPa·s). These MFC are constituted by long and thin fibers arranged in a three-dimensional network interconnected to each other (Molinari et al. 2021).

Preparation of the MFC/plasticizer emulsions and composites

To avoid the MFC agglomeration, cardanol was used as dispersing aid. An emulsion with cardanol, water and MFC was prepared to be fed into the extruder thank to the liquid assisted extrusion technique adopted with success in previous works (Molinari et al. 2021; Aliotta et al. 2023b). The procedure adopted for the liquid assisted extrusion consists of several steps as follows:

- Distilled water was added to MFC, despite their initial dilution, to obtain H₂O/MFC solutions at 2 wt%.
- Cardanol was added to the previous dilution to achieve four different emulsions with the following (H₂O/MFC/CA) ratios by weight: (89.5/0.5/10), (89.25/0.75/10) and (89/1/10).

- The emulsions were then mechanically stirred with an IKA T 25 digital ULTRA-TURRAX® Disperser (Staufen, Germany). The stirring was carried out at 8000 rpm for 210 s to disperse and homogenize the CA with the MFC. The emulsions obtained were stable and does not show phases separation.
- The stable mixed emulsions were then fed through peristaltic pump in proximity of middle length of the twin-screw extrusion system. PLA and PBSA granules in a 60/40 ratio were fed into the extruder through the main feeder located at the beginning of extruder length. The extruder, equipped with a vacuum pumping system that can remove, during the extrusion, the water present in the emulsions, just leaving the plasticizer, MFC and the polymeric PLA/PBSA matrix. A PLA/PBSA matrix with 60 wt.% of PLA and 40wt.% of PBSA was chosen due to its good compromise between processability and mechanical properties (Aliotta et al. 2021, 2023a).

The extrusion compounding was carried out with a semi-industrial COMAC EBC 25HT (L/D=44) twin-screw extruder (COMAC, Cerro Maggiore, Italy). The formulations produced and their relative compositions are reported in Table 1.

The vacuum pump was positioned in proximity of the end of the extruder length to guarantee the maximum stripping yield. The profile temperature adopted along the 11 extruder zones was: 150/170/180/180/180/180/180/190/190/185/180 °C using a mass flow rate of 2.5 kg/h and a screw speed of 100 rpm. The strands coming out from the extruder were cooled in a water bath and then pelletized by an automatic cutter.

Table 1 Blend name and composition

Blend name	PLA/PBSA (60/40) (wt.%)	Cardanol (wt.%)	MFC (wt.%)
PLA_PBSA	100	–	–
10C	90	10	–
10C_0.5MFC	89.5	10	0.5
10C_0.75MFC	89.25	10	0.75
10C_1MFC	89	10	1

FT-IR characterization

To evaluate any eventual interaction between the PLA/PBSA matrix, cardanol and MFC, ATR spectra were recorded on the extruded granules for each blend. The characterization was carried out at room temperature in the 500–4000 cm⁻¹ range using a Nicolet 380 FT-IR spectrometer (Thermo Fisher Scientific, Madison, WI, USA) equipped with a smart iTX ATR accessory.

Rheological characterization of the blends

The dynamic rheological properties of PLA_PBSA, 10C, 10C_0.5MFC, 10C_0.75MFC and 10C_1MFC blends granules were assessed by the rotational ARES rheometer (Rheometric Scientific, New Castle, Delaware, USA), in oscillatory mode from 0.1 to 100 rad/s at 185 °C, using a parallel-plate geometry (diameter=25 mm). The analyses were conducted under nitrogen atmosphere on the granules dried at 70 °C for 12 h in vacuum oven, to prevent moisture degradation. A strain amplitude of 5% was set to ensure the linear viscoelastic regime. The tests were carried out in triplicate yielding a standard deviation below 2%.

Film blowing

Before the film blowing the blend granules were vacuum dried at 70 °C for 12 h. Single layer blown films were produced using a Gimac film blowing unit featuring a single screw extruder (D=12 mm, L/D=24), a spiral mandrel die for blow film (with inner and outer diameters of 30 and 30.5 mm, respectively), and a take-up/cooling system. The films were extruded setting the temperature profile equal to 185/185/175/160 °C, the blow-up ratio (BUR) equal to 2.5 and the collection speed at 1.6 m/min, yielding to samples with an average thickness equal to 45 ± 3 μm. The extrusion proved successful for all the blends compositions except for the 10C sample, which exhibited challenges during blown film processing due to bubble instability. A picture reporting the film processing and the different film formulations produced is reported in Fig. 1.



Fig. 1 Film blowing and related films produced for this work

Morphology

The film morphologies and MFC dispersion were observed by FEI Quanta 450 FEG scanning electron microscope (SEM) (Thermo Fisher Scientific, Waltham, MA, USA). The samples for SEM analyses were cryo-fractured under liquid nitrogen. To avoid some electrostatic charging effects, due to the interaction between the electron beam and the polymeric materials, all the samples were firstly sputtered with a thin layer of platinum by means of LEICA EM ACE 600 High Vacuum Sputter Coater (LEICA, Wetzlar, Germany).

Mechanical characterizations

On the films obtained by film blowing, several mechanical tests were performed. For each test typology, at least five specimens for each formulation were tested.

Tensile tests were carried out on an Instron universal testing machine model 5500R (Canton, MA, USA) equipped with a 100 N load cell interfaced with Merlin software (INSTRON version 4.42 S/N-014733H). Compressed air grips were used to

clamp the film specimens. The specimens consisted of strips having rectangular shape (80 mm length and 15 mm width). The initial grip separation was 50 mm, and the deformation rate was set at 50 mm/min. From this test the final stress and elongation at break of the films was calculated.

The elastic modulus was determined by dynamic mechanical analysis (DMA) carried out on a Gabo Eplexor (Gabo, Ahlden, Germany), equipped with a 100 N load cell. Rectangular specimens were used (gauge length: 20 mm; width: 4 mm). During the test the temperature and the frequency were kept constant and equal to 25 °C and 1 Hz respectively.

The critical tearing energy of the films was evaluated through trouser tear tests carried out with the above mentioned INSTRON universal testing machine.

Trouser tear tests according to the ASTM D1938-02 were carried out at a crosshead speed of 250 mm/min. The “legs” of the trouser specimens were pulled in opposite direction to create a tearing force (mode III of fracture) (Andreasson et al. 2013; Islam et al. 2019). The load and extension values were recorder during the test and the critical tearing energy was calculated as follows:

$$T_C = \frac{2F}{B} \quad (1)$$

where F is the maximum peak load recorded during the test and B is the film thickness.

Tear test at high-speed was carried out thanks to Elmendorf test, a very common test carried out on blown and cast films (Kissin 2011). An Elmendorf pendulum (MESDAN, Puegnago del Garda, Italy) with a weight of 1.6 kg was used and the ISO 6383 was applied to calculate the maximum tearing force. The tests were carried out at room, and the maximum tearing force, in Newton, was registered at higher speeds (50,000 mm/min).

Thermal characterizations

To verify any modification of the thermal properties due to the addition of CA and MFC, calorimetric analysis was performed using a TA-Q200 DSC (TA-Instruments, New Castle, DE) equipped with an RSC cooling system. Indium was used as a standard for the DCS calibration while nitrogen, set at 50 ml/min, was used as purge gas. About 10–15 mg of material, cut from the blown films, was sealed within aluminum hermetic pan. To evaluate the crystallinity reached by the films after the film blowing, only the first heating run was considered. The following thermal program was adopted: heating from 0 at 10 °C/min up to 190 °C. The melting temperature (T_m) and the cold crystallization temperature (T_{cc}) were recorded as the maximum of the melting peak and the minimum of the cold crystallization peak respectively. The enthalpies of melting (ΔH_m) and cold crystallization (ΔH_{cc}) were calculated integrating the areas under the corresponding peaks. The PLA and PBSA crystallinity (X_{cc}) were calculated according to Eq. 2 (Aliotta et al. 2021), where ΔH_m and ΔH_{cc} are the melting and cold crystallization enthalpies respectively. ΔH_m° is the theoretical melting heat of 100% crystalline polymer and it is equal to 93 J/g for PLA (Fischer et al. 1973) and to 142 J/g for PBSA (Burepukdee et al. 2015).

$$X_{cc,PLA(orPBSA)} = \frac{\Delta H_{m,PLA(orPBSA)} - \Delta H_{cc,PLA(orPBSA)}}{\Delta H_{m,PLA(orPBSA)} \cdot \text{wt.\%}PLA(orPBSA)} \quad (2)$$

Oxygen and water vapor barrier characterizations

Oxygen permeability tests were conducted on the films in triplicate, following the ASTM D1434-82 standard, by a GDP-C gas permeabilimeter (Brugger, Munich, Germany) at 23 °C, 10% RH, under an oxygen flow rate of 80 mL/min and at a pressure differential of 1 bar. Permeability coefficients (P_{O_2}) were calculated by multiplying the oxygen transmission rate by the thickness (mm) of each film.

Water vapor permeability measurements were carried out in triple, according to the ASTM F 1249–90 procedure, by a 7002 WP-Permeation Analyzer (Systech Illinois, Princeton, NJ, USA) at 23 °C and 50% RH. Water vapor permeability coefficients (P_{H_2O}) were determined by multiplying the water vapor transmission rate values obtained by the thickness (mm) of each film.

Contact angle measurements

Films wettability was evaluated following the ASTM D5946 standard by static water contact angle measurements, using an FTA 1000 Analyzer (First Ten Angstroms, Inc., Portsmouth, VA, USA) with 2 ± 0.5 μL drop volume and at least ten replicate measurements.

Seal ability characterization

The films sealing ability was assessed according to the ASTM F1921-98, Method B procedure by hot tack tests, using an HSG-C heat seal tester (Brugger, Germany). The welds were performed on 15 mm-width film strips, applying 0.3 N/mm² sealing pressure and 1 s welding time, in the T range from 70 °C, corresponding to the initiation sealing temperature, to 85 °C, above which the film undergoes excessive warping.

Optical properties

The transparency of the films was evaluated with Cary 60 UV–Vis Spectrophotometer (Agilent Technologies, Santa Clara, USA), by measuring the Transmittance % of visible light at 550 nm, according to the ASTM D1746-03 standard.

The color of the films was assessed by colorimeter (CR-4100 Chroma Meter, Konica Minolta, Japan)

and the results were expressed according to CIELAB colour coordinates L^* (darkness/lightness), a^* (greenness/redness), b^* (blueness/yellowness). The colour-difference with respect to the PLA_PBSA film was evaluated using the equation ΔE^*_{ab} , following the standard ASTM D2244.

Results and discussion

Rheological results

Prior to carry out the film blowing process, the blends processability was preliminary investigated by rheological oscillatory analyses. Figure 2 displays the plots of the complex viscosity η^* (a) and storage modulus G' (b) for PLA_PBSA blends, while the

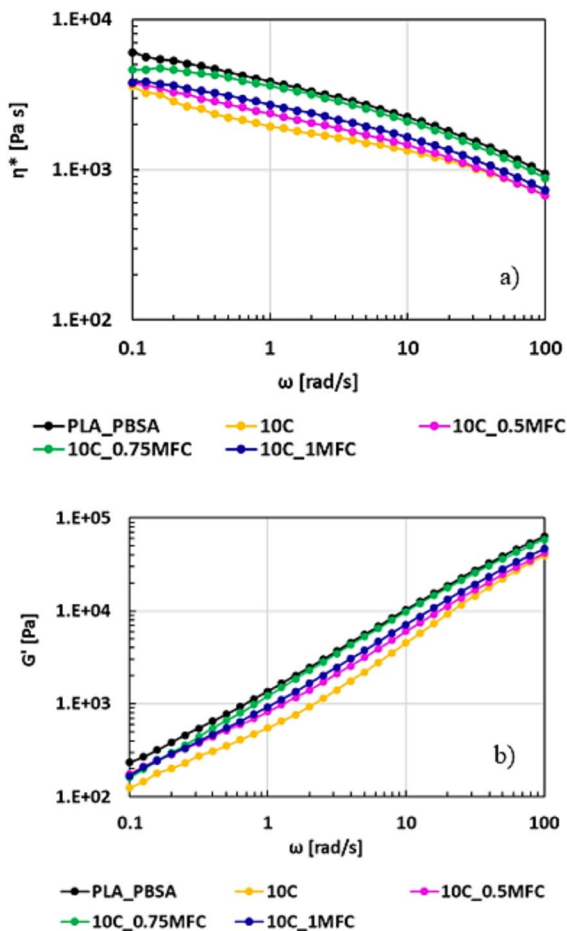


Fig. 2 Complex viscosity curves **a** and storage modulus curves **b** of the PLA_PBSA blends

zero-shear viscosity values are outlined in Table 2. As noticeable from Fig. 2a, all samples exhibit a shear-thinning behavior; the most pronounced is that of the PLA_PBSA matrix, which also shows the highest values of complex viscosity throughout the investigated frequency range.

The addition of cardanol to the polymer matrix (sample 10C) results in a substantial decrease in viscosity: in particular, this sample shows the lowest values of η^* in the entire ω range, while the zero-shear viscosity value (η_0^*), with respect to the PLA_PBSA blend, drops from 6039 to 3581 Pa s.

The decrease in complex viscosity after cardanol oil addition is a typical plasticizing effect. Cardanol acts as plasticizer increasing the free volume and chains mobility of the polymer matrix, as also reported by other authors in literature (Alexander and Thachil 2006; Greco et al. 2019; Mele et al. 2019; Ali et al. 2020).

With respect to the 10C sample, the MFC addition in the blend induces an increase in viscosity. Specifically, for samples loaded with 0.5% and 1% MFC (i.e., 10C_0.5MFC and 10C_1MFC, respectively), only a slight increase in complex viscosities is observed, and the η_0^* values increase from 3581 Pa s, for the 10C sample, to 3735 and 3818 Pa s for the 10C_0.5MFC and 10C_1MFC samples, respectively. On the other hand, the sample loaded at 0.75% MFC (i.e., 10C_0.75 MFC) exhibits the largest increase in viscosity (η_0^* equal to 4595 Pa s) and a more pronounced Newtonian plateau, while at high strain rates (i.e., at high ω values) the complex viscosity approaches that of the neat resin.

These results suggest that the rheological behavior of the composites is strongly correlated to the MFC concentration and its degree of dispersion and distribution in the polymer matrix and can be also interpreted considering SEM analyses, which will be discussed in detail later in the article. In particular, the

Table 2 Zero-shear viscosity values of the PLA_PBSA blends

Blend name	η_0^* [Pa s]
PLA_PBSA	6039
10C	3581
10C_0.5MFC	3735
10C_0.75MFC	4595
10C_1MFC	3818

small viscosity increases in the case of 10C_0.5MFC sample may be associated with a low MFC content coupled with a poor filler distribution as highlighted by SEM analyses. The rheological behavior of sample 10C_0.75MFC suggests that higher interactions between the filler and the polymer matrix were achieved, thanks to a better dispersion and distribution of the filler in the PLA_PBSA matrix. Further increase in MFC percentage up to 1% may induce a worsening in the dispersion and distribution of the filler in the polymer resin, leading to lower complex viscosity values with respect to the 10C_0.75MFC sample.

These observations are also reflected in the storage modulus (G') curves (Fig. 2b). The presence of 10 wt.% of cardanol, plasticizes the matrix causing the highest decrease in the elastic component, which is relevant in the film extrusion process. For samples loaded with MFC, at low strain rates, and therefore for long relaxation times, the plots of G' overlap. At high strain rates, instead, the storage modulus curve of sample 10C_0.75MFC overlaps with that of the neat PLA_PBSA matrix.

Based on the rheological data, the film blowing process was carried out. For sample 10C, the presence of the plasticizer alone made the blown filming process unstable, and it was not possible to collect the film. On the other hand, the enhanced melt elasticity introduced by MFC presence, particularly for concentrations equal to 0.75wt. % and 1 wt.%, ensured a stable film blowing process.

Mechanical and morphological results

The trends of the main mechanical properties (elastic modulus, stress at break and elongation at break) with the overlap of significant stress–strain curves are reported in Fig. 3.

The mechanical results of PLA/PBSA matrix are in accordance with the literature (Yang et al. 2019; Aliotta et al. 2023a). The addition of the more ductile PBSA phase allows the obtention of flexible film having an elongation at break of around 300%. As it could be expected, the addition of the MFC rigid phase, has led to an increment of the film elastic modulus with the MFC content. A slight decrement of

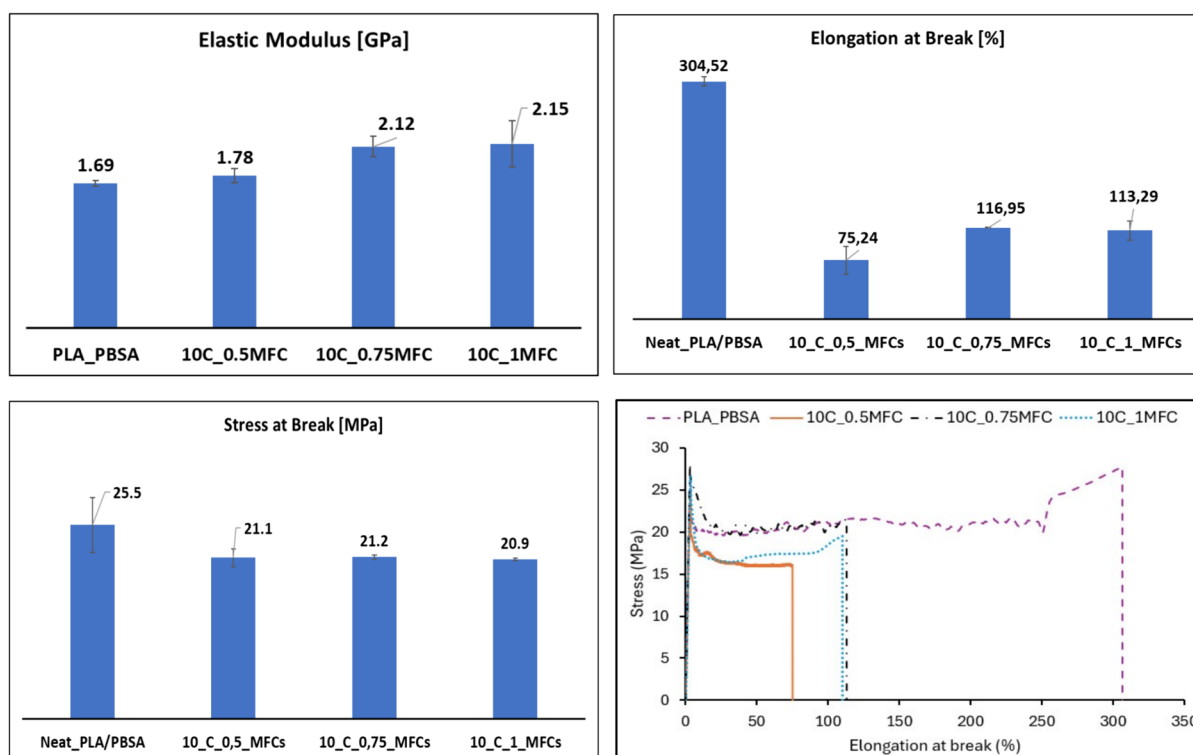


Fig. 3 Mechanical results and relative main stress–strain curves

the stress at break with MFC content was observed; however, this decay is not so marked with values of stress at break that are comparable to the PLA/PBSA matrix. The mechanical results obtained, are in accordance with other studies (Suryanegara et al. 2009; Uribe et al. 2016; Jesus et al. 2022) that ascribed the stiffness increment and the decrement of stress end elongation at break to the presence of the rigid MFC phase. Interesting is to observe the trend of the elongation at break. In fact, even if a decrement of the film's ductility was registered for all biocomposites formulations, the addition of MFC has led to an increment of film ductility. This result could be ascribed to the rigid filler toughening effect caused by the MFC addition (Bartczak et al. 1999). To reach this toughening effect a proper filler content coupled with good dispersion within the polymeric matrix are fundamental (Wilbrink et al. 2001; Argon and Cohen 2003). The highest elongation at break was registered for the composite with 0.75 wt.% MFC content in accordance with the rheological behavior. The MFC content to obtain a flexible film seems to be fundamental. This behavior can be ascribed to a bifurcation phenomenon, reported in literature (Argon and Cohen 2003), between brittle-like response and ductile response that should occur at a critical filler content. At 0.5wt.% of MFC content a brittle response with poor elongation at break was observed. On the other hand, when the MFC content reached the 0.75wt.% the elongation at break started to increase reaching its maximum value.

The tearing resistance of the films evaluated by different techniques and speeds by trouser and Elmendorf tests are reported in Fig. 4. It can be observed that the MFC addition improves the films

tearing resistance. The MFC presence and its good dispersion limits the crack propagation; in fact, if the filler is homogeneously dispersed it can penetrate within polymeric chains and it can limit the slippage of the macromolecules, enhancing the tear resistance (Ismail et al. 2019).

To confirm the mechanical results, the MFC dispersion was checked by SEM analysis (taken at 5000X) and the micrographs obtained are reported in Fig. 5. Unfortunately, it was not possible to go to higher magnifications due to the biopolymeric matrix damage caused by the interaction with the electron beam. However, the micrographs obtained allow to confirm the mechanical results.

The addition of the MFC emulsion containing cardanol changes the morphology of the matrix that has a smoother surface; probably this effect can be ascribed to a sort of plasticization (or compatibilization effect) caused by the CA addition. The increasing MFC content can be observed by the "white dots" (having dimensions around 0.2–0.5 μm) which gradually increase in number, going from 0.5 to 1 wt.% of MFC. It can be also observed that at 0.5 wt.% the MFC content is not enough and there are regions in which only matrix is present. This not enough content coupled with a poor filler distribution, is responsible for the decline in elongation at break recorded for this MFC content. Instead, a suitable content and a more uniform distribution of MFC are visible at 0.75 MFC where an improvement in elongation at break and tear resistance were observed. At 1 wt.% the MFC distribution is still good, however are visible white dots with larger dimensions that are ascribable to the MFC agglomeration.

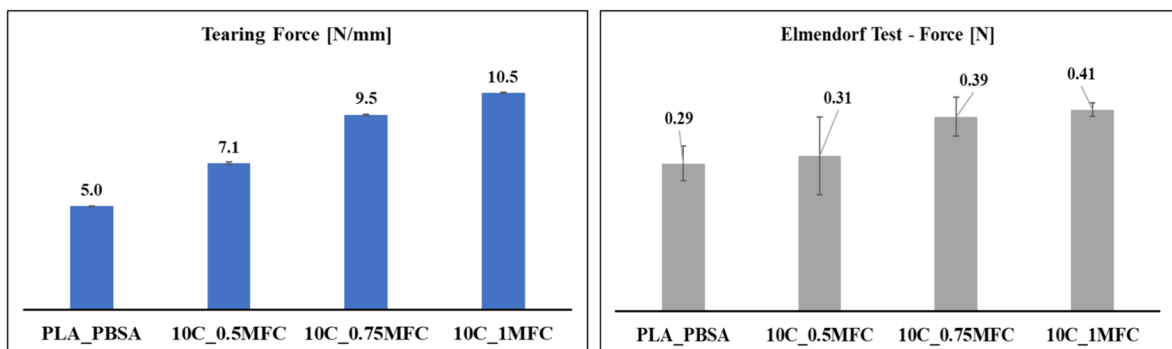


Fig. 4 Results of Trouser tests (left side) and Elmendorf test (right side)

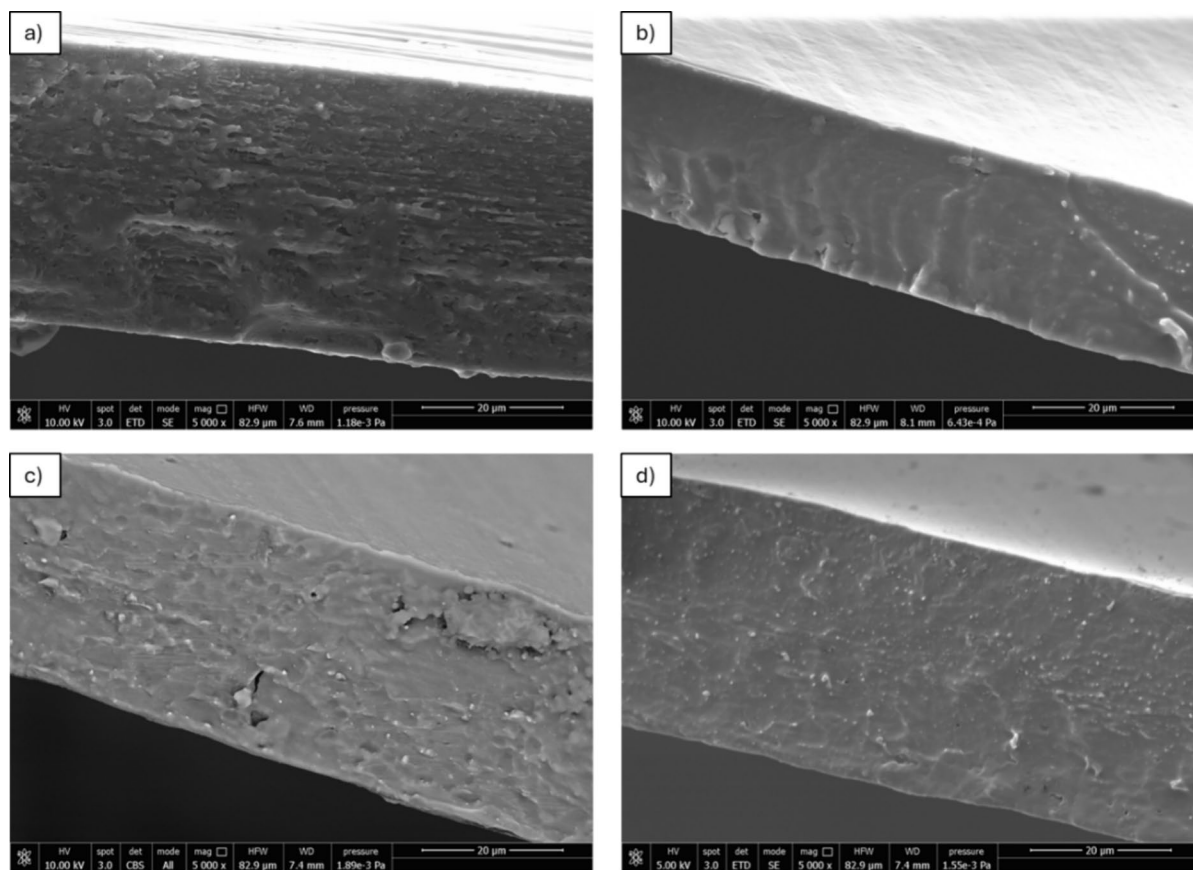


Fig. 5 SEM micrographs at 5000X of **a** PLA_PBSA film and biocomposites films containing **b** 10C_0.5MFC, **c** 10C_0.75MFC and **d** 10C_1MFC

FT-IR results

The FTIR spectra of PLA_PBSA and PLA_PBSA_10C, are reported in Fig. 6a.

For the PLA_PBSA sample, the peaks at 2933 and 2861 cm^{-1} corresponds to characteristics stretching vibration of $-\text{CH}_2$; while the peaks at 1735 cm^{-1} and 1174 cm^{-1} are related to stretching vibration of C=O and C–O, respectively (Palai et al. 2020). The peaks at 1443 cm^{-1} and at 730 cm^{-1} may be ascribed to C–H and C=C main backbone chain of PLA bending of neat PLA, respectively. Similarly, peaks at 1450 and 1382 cm^{-1} may be related to bending of O–H bonds of PBSA carboxylic acid group (Bureepukdee et al. 2015). The addition of cardanol (10C spectrum), is confirmed by the presence of the peak at 1592 cm^{-1} , attributable to the C=C stretching vibration present in the aromatic ring of the molecule (Mestry et al.

2021). A compatibilization effect of cardanol between PLA and PBSA, is here confirmed through the presence of a 1–2 cm^{-1} blue-shift between the two spectra displayed in Fig. 6. This shift can be attributed to the strengthening of the binding energy of the backbone and side groups through inter/intra-molecular interactions (Xie et al. 2016). The blue-shift found here would suggest the existence of an enhanced interaction between the two polymers, thus facilitated by the presence of cardanol.

The FTIR spectra of PLA_PBSA_10C with the addition of different amount of MFC, are reported in Fig. 6b. Here the MFC presence is confirmed by the presence of the peak at 2340 cm^{-1} , generally attributed to the $-\text{N}=\text{C}=\text{O}$ stretching of the polysaccharide (Kaushik and Singh 2011). In addition, it is interesting to notice that as the content of MFC in the sample increases, the area of the peak increases accordingly.

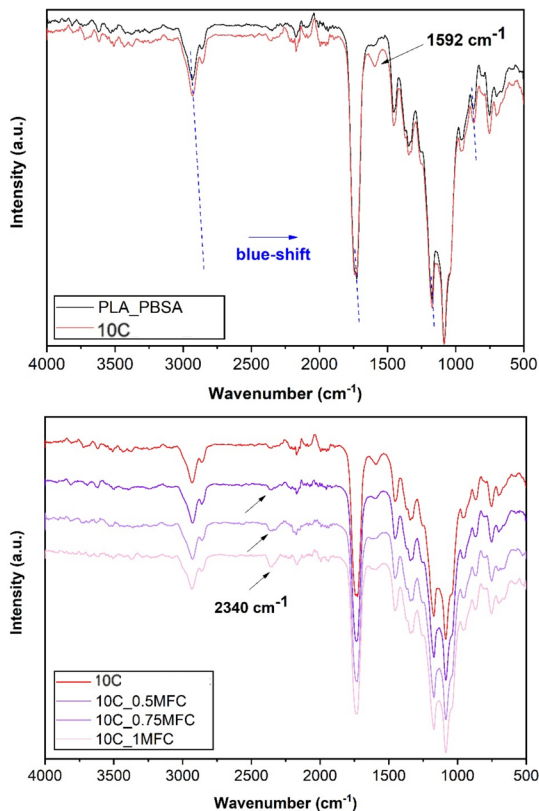


Fig. 6 FTIR spectra of **a** PLA_PBSA and 10C; **b** PLA10C and 10C with the addition of various MFCs amount

Thermal results

In Fig. 7 and Table 3 are reported the heating thermograms and the results obtained from DSC analysis. The first heating thermograms obtained from DSC analysis, shows the thermal history of the samples produced by film blowing. The analysis of these data was preferred to have a better correlation with mechanical results and barrier results measured on the film specimens.

A triple melting peak of PBSA, centered at around 83 °C, is observed. The multiple peak melting behavior is typical for PBSA, also noted in other literature works (Wang et al. 2005; Aliotta et al. 2021). The number of the observable peaks depends on the processing conditions; in fact, according to the melt recrystallization model (Wunderlich 2012), the crystallization temperature and the cooling rate affects the crystals formation generating, in some cases, imperfect crystals having lower melting temperature.

Moreover, during the melting, the amorphous material could recrystallize into a more perfect crystal having high melting temperature. All these phenomena generate multiple melting peak behavior like those observed for PBSA.

The addition of MFC and CA does not significantly affect the PBSA melting. Contrary to PLA, PBSA does not show cold crystallization, this was mainly ascribed to the very fast crystallization rate of PBSA during cooling that leads to the presence of low amorphous domains able to recrystallize during the heating (Bureepukdee et al. 2015). Moreover, the high crystallization rate of PBSA has led to the achievement of crystallinity values (reported in Fig. 7) that remain approximately unchanged with and without the MFC presence. It must be pointed out that the PBSA melting peak is partially overlapped with the PLA cold crystallization peak (centered at around 92 °C) making the calculation of the final crystallinity content less accurate; however, it was possible to calculate the formulations crystallinity trend.

With respect to the PLA/PBSA matrix a marked shift of the PLA melting temperature was observed that passed from 150.8 °C in the matrix to around 155.5 °C in the composites systems. This shift can be ascribed to the MFC presence that acts as nucleating agent and facilitates the crystal formation. In particular, the melting peak shift is ascribed to the formation of only one of the two melting peaks associated to PLA. In fact, it is well known from the literature that PLA has a double melting peak associated to the melt/recrystallization of the PLA α form crystals (Righetti et al. 2015; Aliotta et al. 2017). Depending on the cooling and process conditions, only one or both two peaks are visible. The presence of MFC blurs the peak observed at lower temperatures (recorded for the matrix) and promotes the appearance of a single peak at higher temperatures, consistent with what has also been reported in the literature by Song et al. (Song et al. 2013) for PLA/MFC biocomposites.

In Fig. 8 the crystallinity percentages for PLA, PBSA and the sum of them (that is, the total crystallinity of the sample) are reported.

The fast PBSA crystallization led to high PBSA crystallinity values with and without the MFC presence. On the other hand, the PLA crystallinity increases thank to the presence of MFC that act as heterogeneous nucleating agent for PLA. In fact, PLA

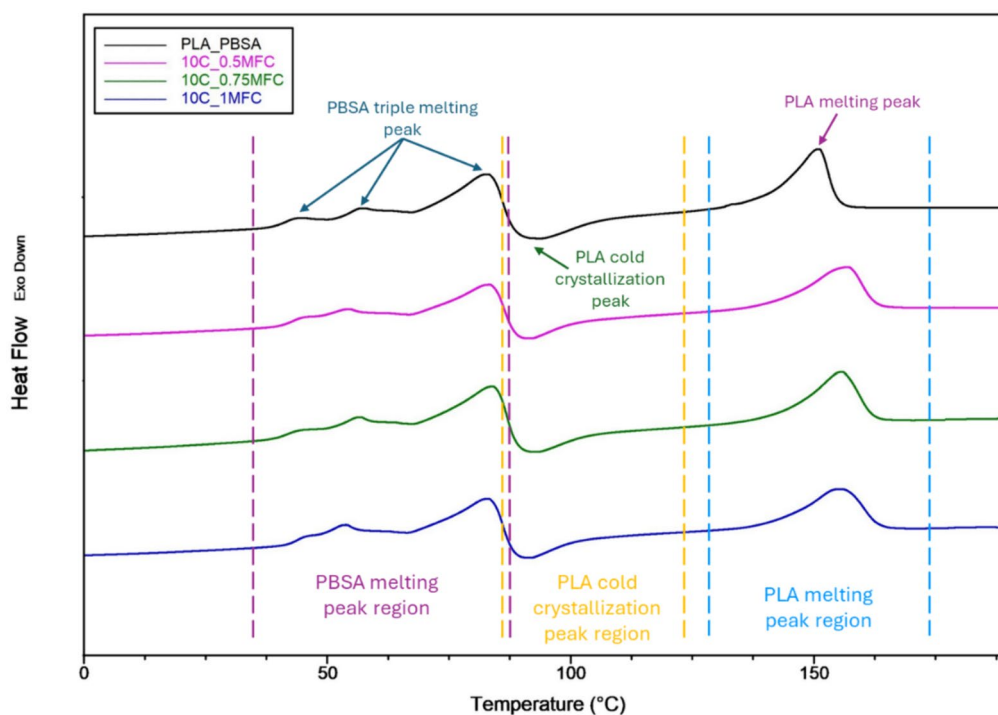
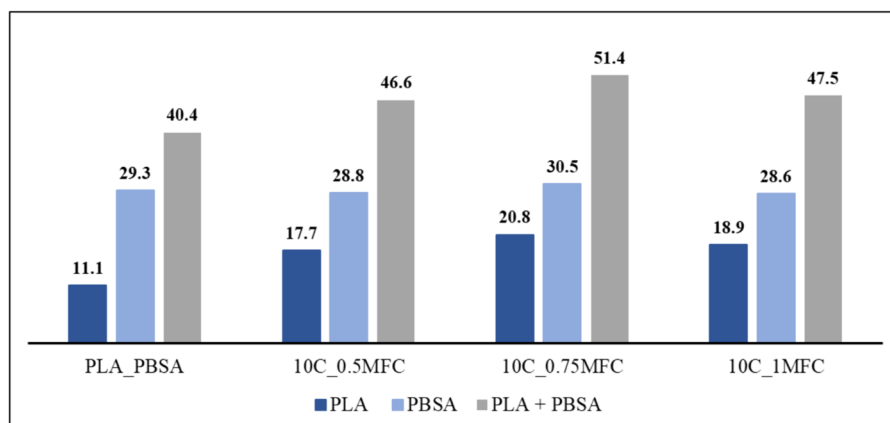


Fig. 7 DSC heating thermograms

Table 3 DSC main results of the first heating

Sample films	$T_{m,PBSA}$ (°C)	$T_{cc,PLA}$ (°C)	$T_{m,PLA}$ (°C)	$\Delta H_{m,PBSA}$ (J/g)	$\Delta H_{cc,PLA}$ (J/g)	$\Delta H_{m,PLA}$ (J/g)
PLA_PBSA	83.0	93.8	151.0	16.6	8.3	14.5
10C_0.5MFC	83.3	90.8	156.9	14.7	5.9	15.8
10C_0.75MFC	83.3	91.7	155.5	15.5	6.0	16.4
10C_1MFC	83.2	91.7	155.4	14.5	7.0	16.4

Fig. 8 Crystallinity values of the film obtained by film blowing technique



has a slower crystallization kinetics and, respect to the matrix without MFC, the MFC addition facilitates its nucleation in accordance with literature (Song et al. 2013). The best MFC content for which the highest PLA crystallinity, and the total composite crystallinity, was reached was equal to 0.75 wt.%.

Oxygen and water vapor barrier and surface wettability

Oxygen and water vapor permeability tests and contact angle measurements were carried out to investigate possible changes in the barrier and surface properties of the films due to MFC addition in the polymer matrix; the outcomes are displayed in Table 4. Both the oxygen and water vapor permeabilities of the neat PLA_PBSA sample are at par or lower than literature data reported for films based on PLA/ polybutylene succinate (PBS), PLA/PBSA, PBS/PBSA blends (Yang et al. 2016; Bamps et al. 2022; Apicella et al. 2023; Jariyasakoolroj et al. 2023). With respect to the PLA_PBSA sample, the incorporation of different percentages of MFC leads to a decrease in the oxygen permeabilities. This effect must be also correlated to the addition of cardanol as MFC dispersing aid that also act as plasticizer for the polymeric matrix increasing the permeability (Mele et al. 2019). However, for samples loaded with 0.5% and 1% MFC only a slight decrease in P_{O_2} values were observed, equal to ca. 4% and 9% for 10C_0.5MFC and 10C_1MFC films, respectively. Conversely, a maximum decrease in P_{O_2} value of 28% was obtained for the 10C_0.75 MFC film. The oxygen barrier results are in close correlation and consistent with the morphological and thermal data discussed before. In detail, the best O_2 -barrier results were found for the 10C_0.75 MFC film, exhibiting a better dispersion and distribution

Table 4 Measured oxygen permeability (P_{O_2}), water vapor permeability (P_{H_2O}), and water contact angle (CA_w) for the tested films

Sample films	$P_{O_2} \left[\frac{cm^3 mm}{m^2 dbar} \right]$	$P_{H_2O} \left[\frac{g mm}{m^2 d} \right]$	$CA_w [^\circ]$
PLA_PBSA	18.4 ± 0.03	0.34 ± 0.04	66.7 ± 1.7
10C_0.5MFC	17.6 ± 1.20	0.48 ± 0.03	72.4 ± 2.5
10C_0.75MFC	13.3 ± 1.40	0.46 ± 0.02	71.6 ± 0.5
10C_1MFC	16.8 ± 1.60	0.49 ± 0.01	69.7 ± 2.7

of the filler in the PLA_PBSA matrix and the highest crystallinity degree achieved for both the PLA and PBSA phases. At the same time, the lower decrease in P_{O_2} of the 10C_0.5MFC and 10C_1MFC films could be attributed to the sub-optimal filler concentration, dispersion, and distribution in the composite matrix, as also underlined by rheological analyses.

Regarding the vapor barrier properties, as was to be expected, a slight increase P_{H_2O} values was observed in the composite structures compared to the pure PLA_PBSA film, with no significant changes with respect to the composition of the films. This is attributable to the inherently hydrophilic nature of MFC due to the high number of hydroxyl groups on its surface, as also reported elsewhere (Jing et al. 2022).

Concerning static water contact angle results (Table 4), in general, composite films show higher CA_w values than the neat PLA_PBSA film; however, this can be reasonably attributed to the presence of the cardanol oil used as a dispersing agent, composed mainly of nonpolar hydrocarbon chains with a phenolic group which makes it relatively hydrophobic. As the concentration of micro-fibrillated cellulose increases, however, the contact angle to water gradually decreases, due to the hydrophilic nature of the filler.

Heat seal performance

The films sealing ability was investigated by evaluating the hot tack strength, namely, the maximum weight the seal can support without breaking, in the temperature range 70–85 °C. The results are displayed in Fig. 9.

All the developed films exhibited a seal initiation temperature equal to 70 °C and a temperature of maximum strength equal to 75 °C. In particular, the neat PLA_PBSA film showed the lowest values of hot tack strength in the whole range of temperatures investigated, and a maximum hot tack strength equal to 850 g/15 mm. By increasing the MFC content in the polymer blend, the hot tack strength gradually increased and a maximum hot tack force equal to 900, 925 and 1000 g/15 mm was registered for 10C_0.5MFC, 10C_0.75MFC and 10C_1MFC samples, respectively. This effect can be explained considering that hot tack is a function of interfacial bonding and melt strength and is more influenced by

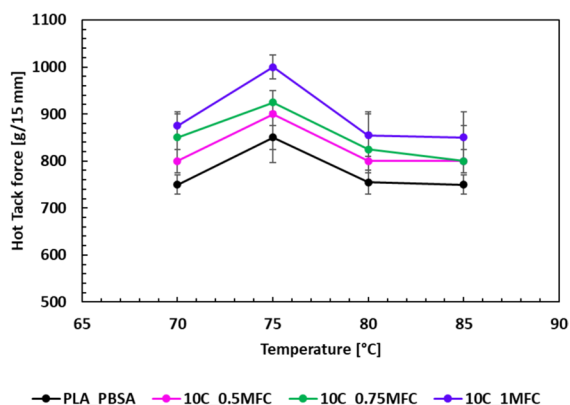


Fig. 9 Hot tack curves for the tested films

Table 5 UV–Vis transmittance at 550 nm (T_{550}) and CieLab color coordinates L^* , a^* and b^* for the tested films. Chromatic variation ΔE^*_{ab} , calculated with respect to the PLA_PBSA film, is also reported

Sample films	T_{550} [%]	L^*	a^*	b^*	ΔE^*_{ab}
PLA_PBSA	78.6	97.5	-0.84	1.65	-
10C_0.5MFC	63.0	97.2	-1.07	2.65	1.1
10C_0.75MFC	63.0	97.5	-1.00	2.50	0.9
10C_1MFC	63.0	97.1	-1.09	2.64	1.1

strong molecular forces than cold adhesion. In particular, the ability of micro-fibrillated cellulose to form stronger bonds, such as hydrogen bonds, can induce an improvement of the interfacial adhesion and of the melt strength, leading to an increased hot tack force by increasing MFC concentration (Morris 2017; Jarvis 2023). It is worth to underline that all the developed films showed a maximum seal strength at $T < 100$ °C, therefore, they can be suitable for applications in high-speed packaging operations (Bamps et al. 2022). What is more, all the films showed maximum seal strength values comparable or higher than those reported in literature for heat sealable, biodegradable films based on PLA, PBS, PBS/PBSA, PLA/polycaprolactone blends (Bamps et al. 2022).

Optical properties

The effect of MFC on the transparency and color of the neat PLA_PBSA and of the composite films was evaluated by UV_Vis and colorimetric measurements.

Table 5 reports the transmission at 550 nm (T_{550}), the CieLab color coordinates L^* , a^* , b^* and the chromatic variation ΔE^*_{ab} for all the films.

As observable, the incorporation of MFC in the PLA_PBSA polymer matrix led to a drop in transparency and a slight increase of the yellowness (b^* parameter) and greenness (a^* parameter) of the films, whereas the L^* parameter remained substantially unchanged. However, no significant changes were noticeable by increasing the MFC concentration from 0.5% up to 1%, and in any case the total color change ΔE^*_{ab} of the composite films, evaluated with respect to the neat PLA_PBSA sample, indicate a minimal or imperceptible difference to the human eye under normal viewing conditions ($\Delta E^*_{ab} \leq 1$).

Conclusions

In this study, biodegradable composite films based on micro fibrillated cellulose were successfully produced by film blowing technique, with the aim to realize a novel structure with improved functional performance suitable for food packaging applications. Different micro fibrillated cellulose (MFC) amount (from 0.5 up to 1 wt.%) was added to the PLA/PBSA matrix, and cardanol oil was employed for the first time as dispersing aid during liquid assisted extrusion.

Cardanol oil was effective in compatibilizing PLA and PBSA and its plasticizing effect substantially decreased the complex viscosity and the storage modulus of the polymer blend, making the film blowing process unstable for the 10C sample. On the contrary, the MFC presence ensured a stable film blowing. Compared to the neat PLA/PBSA sample, the composite films exhibited enhanced oxygen barrier properties, improved hot tack strength without compromising optical characteristics, along with interesting mechanical properties that maintain a good balance between stiffness and ductility. In particular, the 10C_0.75 MFC exhibited a hot tack force equal to 925 g/15 mm and the highest elongation at break (117%) and O₂-barrier ($P_{O_2} = 13.3$ cm² mm/(m² d bar)), attributable to the best dispersion and distribution of the filler in the PLA_PBSA matrix and the highest crystallinity degree achieved for both the PLA and PBSA phases (28.8% and 30.5%, respectively), which hinder the oxygen permeation.

The results obtained highlighted the close relationship between films processing, morphology and the functional performance achieved, are encouraging and underscore the potential of MFC biocomposites in addressing environmental concerns while fulfilling performance requirements in several industrial applications.

Author contributions L.A.: Conceptualization, Methodology, Formal Analysis, Data curation, Visualization, Writing original draft. A.A.: Conceptualization, Methodology, Formal Analysis, Data curation, Visualization, Writing original draft. G.M.: Investigation, Data Curation, Writing—Review & Editing. V.G.: Methodology, Investigation, Data curation, Validation, Writing—Review & Editing. A.P.: Methodology, Investigation, Data curation, Validation, Writing—Review & Editing. L.I.: Validation, Resources, Supervision, Writing—Review & Editing. A.L.: Validation, Resources, Supervision, Writing—Review & Editing.

Funding Open access funding provided by Università di Pisa within the CRUI-CARE Agreement.

Data availability The data supporting this study are available when reasonably requested from the corresponding author.

Declarations

Conflict of interest The authors declare that they have no known competing financial interests or personal relationships that could have appeared to influence the work reported in this paper.

Consent for publication All authors have seen and approved the manuscript.

Open Access This article is licensed under a Creative Commons Attribution 4.0 International License, which permits use, sharing, adaptation, distribution and reproduction in any medium or format, as long as you give appropriate credit to the original author(s) and the source, provide a link to the Creative Commons licence, and indicate if changes were made. The images or other third party material in this article are included in the article's Creative Commons licence, unless indicated otherwise in a credit line to the material. If material is not included in the article's Creative Commons licence and your intended use is not permitted by statutory regulation or exceeds the permitted use, you will need to obtain permission directly from the copyright holder. To view a copy of this licence, visit <http://creativecommons.org/licenses/by/4.0/>.

References

- Alexander M, Thachil ET (2006) A comparative study of cardanol and aromatic oil as plasticizers for carbon-black-filled natural rubber. *J Appl Polym Sci* 102:4835–4841. <https://doi.org/10.1002/app.24811>
- Ali M, Lu Y, Ahmed S et al (2020) Effect of modified cardanol as secondary plasticizer on thermal and mechanical properties of soft polyvinyl chloride. *ACS Omega* 5:17111–17117. <https://doi.org/10.1021/acsomega.0c00826>
- Aliotta L, Cinelli P, Coltelli MB et al (2017) Effect of nucleating agents on crystallinity and properties of poly (lactic acid) (PLA). *Eur Polym J* 93:822–832. <https://doi.org/10.1016/j.eurpolymj.2017.04.041>
- Aliotta L, Vannozi A, Canesi I et al (2021) Poly(lactic acid) (PLA)/Poly(butylene succinate-co-adipate) (PBSA) Compatibilized Binary Biobased Blends: Melt Fluidity, Morphological. *Thermo-Mech Micromech Anal Polym (basel)* 13:218. <https://doi.org/10.3390/polym13020218>
- Aliotta L, Gigante V, Dal Pont B et al (2023a) Tearing fracture of poly(lactic acid) (PLA)/ poly(butylene succinate-co-adipate) (PBSA) cast extruded films: Effect of the PBSA content. *Eng Fract Mech* 289:109450. <https://doi.org/10.1016/j.engfracmech.2023.109450>
- Aliotta L, Gigante V, Molinari G et al (2023b) Effect of biobased plasticizers, used as dispersing aids, on mechanical, rheological and thermal properties of micro fibrillated cellulose (MFC)/poly (lactic acid) (PLA) biocomposites over the time: how MFC controls the plasticizer migration? *Cellulose* 30:2237–2252. <https://doi.org/10.1007/s10570-022-05010-w>
- Anand G, Ravinanthan M, Basaviah R, Av S (2015) In vitro antimicrobial and cytotoxic effects of anacardium occidentale and mangifera indica in oral care. *J Pharm Bioallied Sci* 7:69. <https://doi.org/10.4103/0975-7406.148780>
- de Andrade Jesus Aguiar dos S T, Araújo BQ, das Graças Lopes Citó AM et al (2011) Antioxidant properties and chemical composition of technical cashew nut shell liquid (tCNSL). *Food Chem* 126:1044–1048. <https://doi.org/10.1016/j.foodchem.2010.11.122>
- Andreasson E, Mehmood N, Kao-Walter S (2013) Trouser tear tests of two thin polymer films. In: 13th International Conference on Fracture 2013, ICF 2013. ICF13, pp 4067–4077.
- Apicella A, Scarfato P, Di Maio L et al (2018) Evaluation of performance of PET packaging films based on different copolyester O₂-scavengers. *AIP Conf Proc* 1981:20130. <https://doi.org/10.1063/1.5045992/1027006>
- Apicella A, Scarfato P, Incarnato L (2023) Tailor-made coextruded blown films based on biodegradable blends for hot filling and frozen food packaging. *Food Packag Shelf Life* 37:101096. <https://doi.org/10.1016/J.FPSL.2023.101096>
- Argon AS, Cohen RE (2003) Toughenability of polymers. *Polymer (guildf)* 44:6013–6032. [https://doi.org/10.1016/S0032-3861\(03\)00546-9](https://doi.org/10.1016/S0032-3861(03)00546-9)
- Augé M-O, Roncucci D, Bourbigot S et al (2023) Recent advances on reactive extrusion of Poly(lactic acid). *Eur Polym J* 184:111727. <https://doi.org/10.1016/j.eurpolymj.2022.111727>
- Aversa C, Cappiello G, Barletta M (2022) Study of binary PLA/PBSA and ternary blends PLA/PCL/PBSA for the manufacturing of single dose strips. *Procedia CIRP* 110:335–341. <https://doi.org/10.1016/j.procir.2022.06.060>

- Bamps B, Guimaraes RMM, Duijsters G et al (2022) Characterizing mechanical, heat seal, and gas barrier performance of biodegradable films to determine food packaging applications. *Polymers (basel)* 14:2569. <https://doi.org/10.3390/polym14132569>
- Bartczak Z, Argon AS, Cohen RE, Weinberg M (1999) Toughness mechanism in semi-crystalline polymer blends: I high-density polyethylene toughened with rubbers. *Polymer (guildf)* 40:2331–2346. [https://doi.org/10.1016/S0032-3861\(98\)00445-5](https://doi.org/10.1016/S0032-3861(98)00445-5)
- Bloise E, Carbone L, Colafemmina G et al (2012) First example of a lipophilic porphyrin-cardanol hybrid embedded in a cardanol-based micellar nanodispersion. *Molecules* 17:12252–12261. <https://doi.org/10.3390/molecules171012252>
- Boonsai P, Phuwapraisirisan P, Chanchao C (2014) Antibacterial activity of a cardanol from thai apis mellifera propolis. *Int J Med Sci* 11:327–336. <https://doi.org/10.7150/ijms.7373>
- Botta L, Teresi R, Titone V et al (2021) Use of biochar as filler for biocomposite blown films: structure-processing-properties relationships. *Polymers (basel)* 13:3953. <https://doi.org/10.3390/polym13223953>
- Bureepukdee C, Suttiruengwong S, Seadan M (2015) A study on reactive blending of (poly lactic acid) and poly (butylene succinate co adipate). *IOP Conf Ser Mater Sci Eng* 87:012070. <https://doi.org/10.1088/1757-899X/87/1/012070>
- Changwichan K, Silalertruksa T, Gheewala S (2018) Eco-efficiency assessment of bioplastics production systems and end-of-life options. *Sustainability* 10:952. <https://doi.org/10.3390/su10040952>
- Clemons C, Sabo R (2021) A review of wet compounding of cellulose nanocomposites. *Polymers (basel)* 13:911. <https://doi.org/10.3390/polym13060911>
- De Luca S, Milanese D, Gallichi-Nottiani D et al (2023) Poly(lactic acid) and its blends for packaging application: a review. *Clean Technol* 5:1304–1343. <https://doi.org/10.3390/cleantechnol5040066>
- de Sousa FDB (2021) The role of plastic concerning the sustainable development goals: the literature point of view. *Clean Respons Consum* 3:100020. <https://doi.org/10.1016/j.clrc.2021.100020>
- Dörnyei KR, Uysal-Unalan I, Krauter V et al (2023) Sustainable food packaging: an updated definition following a holistic approach. *Front Sustain Food Syst* 7:1119052. <https://doi.org/10.3389/fsufs.2023.1119052>
- Dufresne A (2017) Cellulose nanomaterial reinforced polymer nanocomposites. *Curr Opin Colloid Interface Sci* 29:1–8. <https://doi.org/10.1016/j.cocis.2017.01.004>
- Evstatiev M, Fakirov S (1992) Microfibrillar reinforcement of polymer blends. *Polymer (guildf)* 33:877–880. [https://doi.org/10.1016/0032-3861\(92\)90354-Y](https://doi.org/10.1016/0032-3861(92)90354-Y)
- Fischer EW, Sterzel HJ, Wegner G (1973) Investigation of the structure of solution grown crystals of lactide copolymers by means of chemical reactions. *Kolloid-Zeitschrift Zeitschrift Für Polym* 251:980–990. <https://doi.org/10.1007/BF01498927>
- Gigante V, Aliotta L, Dal Pont B et al (2023) Tailoring morphology and mechanical properties of PLA/PBSA blends optimizing the twin-screw extrusion processing parameters aided by a 1D simulation software. *Polym Test* 129:108294. <https://doi.org/10.1016/j.polymertesting.2023.108294>
- Greco A, Ferrari F, Maffezzoli A (2018) Thermal analysis of poly(lactic acid) plasticized by cardanol derivatives. *J Therm Anal Calorim* 134:559–565. <https://doi.org/10.1007/S10973-018-7059-4/FIGURES/8>
- Greco A, Ferrari F, Maffezzoli A (2019) Mechanical properties of poly(lactic acid) plasticized by cardanol derivatives. *Polym Degrad Stab* 159:199–204. <https://doi.org/10.1016/j.polymdegradstab.2018.11.028>
- Hassouma F, Mihai I, Fetzer L et al (2016) Design of new cardanol derivative: synthesis and application as potential biobased plasticizer for poly(lactide). *Macromol Mater Eng* 301:1267–1278. <https://doi.org/10.1002/MAME.201600190>
- Islam MS, Andreasson E, Kao-Walter S (2019) Trouser tear testing of thin anisotropic polymer films and laminates. *Int J Fract* 219:187–201. <https://doi.org/10.1007/s10704-019-00389-3>
- Ismail I, Osman AF, Ping TL (2019) Effects of ultrasonication process on crystallinity and tear strength of thermoplastic starch/cellulose biocomposites. *IOP Conf Ser Mater Sci Eng* 701:012045. <https://doi.org/10.1088/1757-899X/701/1/012045>
- Jariyasakoolroj P, Klairasamee K, Kumsang P et al (2023) Effect of Biaxial orientation on gas permeability and remarkably enhanced toughness of Poly(butylene succinate)-based films. *J Polym Environ*. <https://doi.org/10.1007/s10924-023-03085-5>
- Jarvis MC (2023) Hydrogen bonding and other non-covalent interactions at the surfaces of cellulose microfibrils. *Cellulose* 30:667–687. <https://doi.org/10.1007/s10570-022-04954-3>
- Jesus LCC, Oliveira JM, Leão RM et al (2022) Tensile behavior analysis combined with digital image correlation and mechanical and thermal properties of microfibrillated cellulose fiber/poly(lactic acid) composites. *Polym Test* 113:107665. <https://doi.org/10.1016/j.polymertesting.2022.107665>
- Jing M, Zhang L, Fan Z et al (2022) Markedly improved hydrophobicity of cellulose film via a simple one-step aminosilane-assisted ball milling. *Carbohydr Polym* 275:118701. <https://doi.org/10.1016/J.CARBPOL.2021.118701>
- Kalia S, Dufresne A, Cherian BM et al (2011) Cellulose-based bio- and nanocomposites: a review. *Int J Polym Sci* 2011:1–35. <https://doi.org/10.1155/2011/837875>
- Kaushik A, Singh M (2011) Isolation and characterization of cellulose nanofibrils from wheat straw using steam explosion coupled with high shear homogenization. *Carbohydr Res* 346:76–85. <https://doi.org/10.1016/j.carres.2010.10.020>
- Kissin YV (2011) Elmendorf tear test of polyethylene films: mechanical interpretation and model. *Macromol Mater Eng* 296:729–743. <https://doi.org/10.1002/MAME.20100419>
- Lamm ME, Li K, Qian J et al (2021) Recent advances in functional materials through cellulose nanofiber templating. *Adv Mater* 33:2005538. <https://doi.org/10.1002/ADMA.202005538>

- Lascano D, Quiles-Carrillo L, Balart R et al (2019) Toughened poly (lactic acid)-PLA formulations by binary blends with poly(butylene succinate-co-adipate)-PBSA and their shape memory behaviour. *Materials* 12:1–14. <https://doi.org/10.3390/ma12040622>
- Leneveu-Jenvrin C, Apicella A, Bradley K et al (2021) Effects of maturity level, steam treatment, or active packaging to maintain the quality of minimally processed mango (*Mangifera indica* cv. José). *J Food Process Preserv* 45:e15600. <https://doi.org/10.1111/JFPP.15600>
- Li K, Mcgrady D, Zhao X et al (2021) Surface-modified and oven-dried microfibrillated cellulose reinforced biocomposites: cellulose network enabled high performance. *Carbohydr Polym* 256:117525. <https://doi.org/10.1016/j.carbpol.2020.117525>
- Malafeev KV, Apicella A, Incarnato L, Scarfato P (2023) Understanding the impact of biodegradable microplastics on living organisms entering the food chain: a review. *Polymers (basel)* 15:3680. <https://doi.org/10.3390/polym15183680>
- Marcilla A, Garcia JC, Beltran M (2017) Plasticizers in various industrial products. In: Wypych G (ed) *Handbook of plasticizers*. Elsevier, pp 495–605
- Mastalygina EE, Aleksanyan KV (2023) Recent approaches to the plasticization of poly(lactic acid) (PLA) (a review). *Polymers (basel)* 16:87. <https://doi.org/10.3390/polym16010087>
- Mele G, Bloise E, Cosentino F et al (2019) Influence of cardanol oil on the properties of poly(lactic acid) films produced by melt extrusion. *ACS Omega* 4:718–726. <https://doi.org/10.1021/acsomega.8b02880>
- Mestry SU, Khuntia SP, Mhaske ST (2021) Development of waterborne polyurethane dispersions (WPUdS) from novel cardanol-based reactive dispersing agent. *Polym Bull* 78:6819–6834. <https://doi.org/10.1007/s00289-020-03450-7>
- Molinari G, Gigante V, Fiori S et al (2021) Dispersion of micro fibrillated cellulose (MFC) in poly(lactic acid) (PLA) from lab-scale to semi-industrial processing using biobased plasticizers as dispersing aids. *Chemistry (easton)* 3:896–915. <https://doi.org/10.3390/chemistry3030066>
- Morris BA (2017) Introduction. In: Morris BA (ed) *The science and technology of flexible packaging* 1st edition. Elsevier, UK, p 179
- Nath D, Pal AK, Misra M, Mohanty AK (2023) Biodegradable blown film composites from bioplastic and talc: effect of uniaxial stretching on mechanical and barrier properties. *Macromol Mater Eng* 308:2300214. <https://doi.org/10.1002/mame.202300214>
- Nofar M, Sacligil D, Carreau PJ et al (2019) Poly (lactic acid) blends: processing, properties and applications. *Int J Biol Macromol* 125:307–360. <https://doi.org/10.1016/j.ijbiomac.2018.12.002>
- Palai B, Mohanty S, Nayak SK (2020) Synergistic effect of polylactic acid(PLA) and poly(butylene succinate-co-adipate) (PBSA) based sustainable, reactive, super toughened eco-composite blown films for flexible packaging applications. *Polym Test* 83:106130. <https://doi.org/10.1016/J.POLYMERTESTING.2019.106130>
- Paul UC, Fragouli D, Bayer IS et al (2021) Effect of green plasticizer on the performance of microcrystalline cellulose/polylactic acid biocomposites. *ACS Appl Polym Mater* 3:3071–3081. <https://doi.org/10.1021/acsapm.1c00281>
- Pivsa-Art W, Pivsa-Art S, Fujii K et al (2015) Compression molding and melt-spinning of the blends of poly(lactic acid) and poly(butylene succinate-co-adipate). *J Appl Polym Sci* 132:41856. <https://doi.org/10.1002/app.41856>
- Qian S, Sheng K (2017) PLA toughened by bamboo cellulose nanowhiskers: role of silane compatibilization on the PLA bionanocomposite properties. *Compos Sci Technol* 148:59–69. <https://doi.org/10.1016/j.compscitech.2017.05.020>
- Righetti MC, Gazzano M, Di Lorenzo ML, Androsch R (2015) Enthalpy of melting of α' - and α -crystals of poly(l-lactic acid). *Eur Polym J* 70:215–220. <https://doi.org/10.1016/j.eurpolymj.2015.07.024>
- Samir A, Ashour FH, Hakim AAA, Bassyouni M (2022) Recent advances in biodegradable polymers for sustainable applications. *Npj Mater Degrad* 6:68. <https://doi.org/10.1038/s41529-022-00277-7>
- Song Y, Tashiro K, Xu D et al (2013) Crystallization behavior of poly(lactic acid)/microfibrillated cellulose composite. *Polymer (guildf)* 54:3417–3425. <https://doi.org/10.1016/j.polymer.2013.04.054>
- Stark NM, Matuana LM (2021) Trends in sustainable biobased packaging materials: a mini review. *Mater Today Sustain* 15:100084. <https://doi.org/10.1016/j.mtsust.2021.100084>
- Suryanegara L, Nakagaito AN, Yano H (2009) The effect of crystallization of PLA on the thermal and mechanical properties of microfibrillated cellulose-reinforced PLA composites. *Compos Sci Technol* 69:1187–1192. <https://doi.org/10.1016/j.compscitech.2009.02.022>
- Suwanamornlert P, Kerddonfag N, Sane A et al (2020) Poly(lactic acid)/poly(butylene-succinate-co-adipate) (PLA/PBSA) blend films containing thymol as alternative to synthetic preservatives for active packaging of bread. *Food Packag Shelf Life* 25:100515. <https://doi.org/10.1016/j.fpsl.2020.100515>
- Swetha TA, Ananthi V, Bora A et al (2023) A review on biodegradable polylactic acid (PLA) production from fermentative food waste-Its applications and degradation. *Int J Biol Macromol* 234:123703. <https://doi.org/10.1016/j.ijbiomac.2023.123703>
- Uribe BEB, Carvalho AJF, Tarpani JR (2016) Low-cost, environmentally friendly route to produce glass fiber-reinforced polymer composites with microfibrillated cellulose interphase. *J Appl Polym Sci* 133:44183. <https://doi.org/10.1002/app.44183>
- van den Oever MJA, Beck B, Müssig J (2010) Agrofibre reinforced poly(lactic acid) composites: effect of moisture on degradation and mechanical properties. *Compos Part A Appl Sci Manuf* 41:1628–1635. <https://doi.org/10.1016/j.compositesa.2010.07.011>
- Völtz LR, Geng S, Teleman A, Oksman K (2022) Influence of dispersion and orientation on polyamide-6 cellulose nanocomposites manufactured through liquid-assisted extrusion. *Nanomaterials* 12:818. <https://doi.org/10.3390/nano12050818>

- Wang Y, Bhattacharya M, Mano JF (2005) Thermal analysis of the multiple melting behavior of poly(butylene succinate-co-adipate). *J Polym Sci B Polym Phys* 43:3077–3082. <https://doi.org/10.1002/polb.20589>
- Wilbrink MWL, Argon AS, Cohen RE, Weinberg M (2001) Toughenability of Nylon-6 with CaCO₃ filler particles: new findings and general principles. *Polymer (guildf)* 42:10155–10180. [https://doi.org/10.1016/S0032-3861\(01\)00548-1](https://doi.org/10.1016/S0032-3861(01)00548-1)
- Wunderlich B (2012) *Macromolecular physics*. Elsevier
- Xie L, Xu H, Niu B et al (2014) Unprecedented access to strong and ductile poly(lactic acid) by introducing in situ nanofibrillar poly(butylene succinate) for green packaging. *Biomacromol* 15:4054–4064. <https://doi.org/10.1021/bm5010993>
- Xie L, Xu H, Li L Bin, et al (2016) Biomimetic nanofibrillation in two-component biopolymer blends with structural analogs to spider silk. *Scientific Reports* 2016, 6:1–11. <https://doi.org/10.1038/srep34572>
- Yang X, Xu H, Odelius K, Hakkarainen M (2016) Poly(lactide)-g-poly(butylene succinate-co-adipate) with high crystallization capacity and migration resistance. *Materials* 9:313. <https://doi.org/10.3390/ma9050313>
- Yang C, Tang H, Wang Y et al (2019) Development of PLA-PBSA based biodegradable active film and its application to salmon slices. *Food Packag Shelf Life* 22:100393. <https://doi.org/10.1016/j.fpsl.2019.100393>
- Zinoviadou KG, Gougouli M, Biliaderis CG (2016) Innovative biobased materials for packaging sustainability. In: Galanakis CM (ed) *Innovation strategies in the food industry*. Elsevier, pp 167–189

Publisher's Note Springer Nature remains neutral with regard to jurisdictional claims in published maps and institutional affiliations.